





Listerin promotes cGAS protein degradation through the ESCRT pathway to negatively regulate cGAS-mediated immune response

Fei Qin^{a,b}, Baoshan Cai^{a,b}, Runyu Cao^{a,b}, Xuemei Bai^{a,b}, Jiahua Yuan^{a,b}, Yuling Zhang^{a,b}, Yaxing Liu^{a,b}, Tian Chen^{a,c}, Feng Liu^{a,b}, Wanwei Sun^{a,b} , Yi Zheng^{a,b}, Xiaopeng Qi^d, Wei Zhao^{a,c} , Bingyu Liu^{a,b,1}, and Chengjiang Gao^{a,b,1}

Edited by Veit Hornung, Ludwig-Maximilians-Universität München Department Biochemie, Munich, Germany; received June 2, 2023; accepted October 27, 2023 by Editorial Board Member Carl F. Nathan

The enzyme cyclic GMP-AMP synthase (cGAS) is a key sensor for detecting misplaced double-stranded DNA (dsDNA) of genomic, mitochondrial, and microbial origin. It synthesizes 2'3'-cGAMP, which in turn activates the stimulator of interferon genes pathway, leading to the initiation of innate immune responses. Here, we identified Listerin as a negative regulator of cGAS-mediated innate immune response. We found that Listerin interacts with cGAS on endosomes and promotes its K63-linked ubiquitination through recruitment of the E3 ligase TRIM27. The polyubiquitinated cGAS is then recognized by the endosomal sorting complexes required for transport machinery and sorted into endosomes for degradation. Listerin deficiency enhances the innate antiviral response to herpes simplex virus 1 infection. Genetic deletion of Listerin also deteriorates the neuroinflammation and the ALS disease progress in an ALS mice model; overexpression of Listerin can robustly ameliorate disease progression in ALS mice. Thus, our work uncovers a mechanism for cGAS regulation and suggests that Listerin may be a promising therapeutic target for ALS disease.

cGAS | ESCRT | antiviral innate immunity | listerin | ALS

The innate immune system detects danger signals, such as molecular patterns from pathogens or tissue damage, through various pattern-recognition receptors (PRRs) (1). The presence of cytosolic DNA serves as the essential danger signal for pathogen infection and initiates strong immune responses (2–4). cGAS (cyclic GMP-AMP synthase) is a pivotal intracellular PRR that detects microbial DNA or self-DNA in the cytoplasm. Upon DNA recognition, cGAS can rearrange its catalytic pocket structure and undergo oligomerization, which effectively catalyzes ATP and GTP to synthesize the second messenger 2'3'-cyclic GMP-AMP (cGAMP) (5, 6). The cGAMP binds to the stimulator of interferon genes (STING), which translocates from the endoplasmic reticulum to the Golgi apparatus, where it initiates downstream pathways through Tank-binding kinase 1 (TBK1) and Interferon regulatory factor 3 (IRF3), resulting in the production of type I interferons (IFNs) and other pro-inflammatory cytokines (7, 8).

Although this surveillance system serves as a widespread and effective defense mechanism against tissue damage and invasion by pathogens, aberrant activation of cGAS by self DNA significantly contributes to several severe neurodegenerative disorders. For example, TDP-43 abnormalities may affect the stability and integrity of mtDNA, leading to the release of mtDNA into the cytoplasm. These leaked mtDNA can activate cGAS and induce the immune response and inflammation in ALS pathology (9). Several studies have reported that abnormal DNA damage in mouse models of Alzheimer's disease (AD) can induce the activation of the cGAS–STING signaling, which subsequently exacerbates neuroinflammation and worsens the progression of AD pathology and cognitive decline (10–12). In Parkinson's disease (PD), nitric oxide stress caused by increased pathologic α -syn aggregates leads to the activation of cGAS/STING from genomic DNA double-strand breaks, which exacerbates pathologic neuroinflammation in patients with PD (13). Thus, inhibition of cGAS offers potential therapeutic benefits for these neurodegenerative diseases.

Ubiquitination is the process in which a 76-amino acid protein called ubiquitin is covalently attached to the target protein substrate. This process is mediated by E1, E2, and E3 enzymes and serves as a signal for protein degradation (14, 15). The endosomal sorting complexes required for transport (ESCRT) system can capture ubiquitinated proteins and subsequently sequester them into intraluminal vesicles (ILVs) contained within the late endosome, which ultimately fuse with lysosomes for protein degradation (16). The ESCRT pathway consists of four complexes (ESCRT-0, ESCRT-I, ESCRT-II, and

Significance

The cyclic guanosine monophosphate (GMP)-adenosine monophosphate (AMP) (cGAMP) synthase (cGAS) is a key sensor for detecting misplaced double-stranded DNA. The timely degradation of cGAS is essential to maintain cell homeostasis. Whether the ESCRT (endosomal sorting complexes required for transport) system regulates cGAS degradation is currently unknown. In this study, we found that Listerin is responsible for recruiting TRIM27 to initiate K63-linked polyubiquitination of cGAS, which subsequently facilitates the sorting and degradation of cGAS on the endosome via an ESCRT-dependent pathway. Moreover, Listerin-deficient mice showed more severe amyotrophic lateral sclerosis (ALS)-related neurobehavioral symptoms and increased neuroinflammation. Targeting Listerin to alleviate inflammation resulting from the overactivation of the cGAS–STING (stimulator of interferon genes) signaling pathway represents a promising therapeutic strategy.

This article is a PNAS Direct Submission. V.H. is a guest editor invited by the Editorial Board.

Copyright © 2023 the Author(s). Published by PNAS. This article is distributed under [Creative Commons Attribution-NonCommercial-NoDerivatives License 4.0 \(CC BY-NC-ND\)](https://creativecommons.org/licenses/by-nc-nd/4.0/).

¹To whom correspondence may be addressed. Email: liubingyu@sdu.edu.cn or cgao@sdu.edu.cn.

This article contains supporting information online at <https://www.pnas.org/lookup/suppl/doi:10.1073/pnas.2308853120/-/DCSupplemental>.

Published December 18, 2023.

ESCRT-III) that function sequentially to sort ubiquitinated proteins into ILVs within multivesicular bodies (MVBs). The ESCRT-0 complex recognizes ubiquitinated proteins and recruits the ESCRT-I and ESCRT-II complexes to the endosomal membrane. The ESCRT-III complex also mediates the final step of membrane fission, separating the ILVs from the MVB limiting membrane and subsequently fusing with the lysosome, leading to ubiquitination degradation (17, 18). Three recent studies almost simultaneously reported that ubiquitinated STING protein could lead to its degradation through ESCRT machinery, which results in the cessation of STING-mediated signaling. They all emphasized that STING was modified by K63 ubiquitination as the initiating factor of this process (19–21). These findings suggest that the ESCRT complex may modulate innate antiviral signaling; however, whether the ESCRT system regulates cGAS degradation is currently unknown.

Our results demonstrate that the ESCRT pathway is involved in the degradation of cGAS proteins. We found that the Ribosome-associated protein quality control (RQC) component Listerin is responsible for recruiting TRIM27 to initiate K63-linked polyubiquitination of cGAS, which subsequently facilitates the sorting and degradation of cGAS proteins on the endosome via an ESCRT-dependent pathway. Furthermore, Listerin deficiency leads to an increased production of IFNs and promotes innate antiviral response to DNA virus infection both in vitro and in vivo. Furthermore, the overexpression of Listerin is found to mitigate TDP-43-induced neuroinflammation and ameliorate neurobehavioral symptoms in ALS mice. This study reveals Listerin as a potential therapeutic target for neurodegenerative diseases, offering promising avenues for the development of new therapeutic approaches in the future.

Results

Listerin Deficiency Promotes the cGAS–STING Activation. The cGAS–STING pathway has emerged as a critical player in a wide range of diseases and dysregulation or aberrant activation of this pathway may trigger different conditions mainly through regulating the production of IFN- β and a variety of inflammatory factors (22). The process of Ribosome-associated protein RQC serves as a mechanism for monitoring proteins and removing faulty nascent polypeptides. Listerin, an E3 ubiquitin ligase, plays a crucial role in regulating RQC by identifying and marking substrates for ubiquitination. The involvement of Listerin in immune responses has not yet been reported (23, 24).

To investigate the potential regulatory roles of Listerin in cGAS–STING pathway, we designed specific siRNA targeting Listerin to knock down the expression of endogenous Listerin in mouse macrophages (SI Appendix, Fig. S1A). Small interfering RNA (siRNA)-mediated silencing of Listerin in macrophages caused an increase in HSV-1 (herpes simplex virus 1) virus infection- or interferon-stimulating DNA (ISD)-induced mRNA levels of *Ifnb1*, as well as IFN- β protein secretion (SI Appendix, Fig. S1B). However, stimulation with cGAMP, the endogenous STING ligand, did not increase the type I IFNs production. (SI Appendix, Fig. S1B). Knockdown of Listerin in human THP-1 cells also promoted ISD-induced mRNA levels of *IFNB1* and *IFNA4*, but not cGAMP (SI Appendix, Fig. S1 C and D). These data indicated that Listerin may regulate the cGAS-mediated type I IFNs production.

To further investigate the roles of Listerin in the cGAS–STING pathway, we generated Listerin knockout mice specifically in myeloid cells by crossing *Listerin*^{fl/fl} mice with *Lyz2-Cre* mice. Similar to the siRNA knockdown results, we observed increased mRNA

levels of *Ifnb1* and *Ifna4*, as well as IFN- β protein level, in *Listerin*^{fl/fl} *Lyz2-Cre* macrophages compared to *Listerin*^{fl/fl} macrophages upon stimulation with HSV-1 virus or ISD (Fig. 1 A and B). Similarly, our data showed that Listerin knockout had no regulatory effects on the type I IFNs production by stimulation with cGAMP (Fig. 1C). Moreover, we cultured bone marrow-derived macrophages and observed higher mRNA levels of *Ifnb1* and *Ifna4* in *Listerin*^{fl/fl} *Lyz2-Cre* macrophages compared to *Listerin*^{fl/fl} macrophages after ISD stimulation, while there was no change in cGAMP stimulation (SI Appendix, Fig. S1E). Furthermore, we generated the Listerin-knockout HeLa cell line using CRISPR-Cas9-mediated gene targeting and found that knockout of Listerin in HeLa cells increased *IFNB1* mRNA levels after HSV-1 infection (Fig. 1D). In contrast, we observed a decrease in the expression of *IFNB1* mRNA induced by HSV-1 infection or ISD stimulation after overexpression of the Flag-Listerin plasmid in HeLa cells, as compared to transfection with an empty vector (Fig. 1 E and F). We repeated the overexpression experiments in MEF cells and obtained the similar results as seen in HeLa cells (SI Appendix, Fig. S1F). Moreover, we cultured the human induced pluripotent stem cells (iPSCs) and generated iPSC-derived microglia; following adenovirus-mediated overexpression of Listerin, we observed that HSV-1 infection or ISD stimulation induced decreased expression of *IFNB1* mRNA in iPSC-derived microglia (SI Appendix, Fig. S1G). HSV-1 or ISD induced increased IFN- β protein secretion was higher after overexpression of Listerin in iPSC-derived microglia (SI Appendix, Fig. S1H).

The cGAS–STING pathway operates primarily through the activation of TBK1 and transcription factors of IRF3 and NF- κ B to regulate the type I IFN production. Compared to *Listerin*^{fl/fl} macrophages, we found increased phosphorylation of TBK1, IRF3, and P65 in *Listerin*^{fl/fl} *Lyz2-Cre* macrophages following HSV-1 infection or ISD stimulation (Fig. 1 G–J). We detected that cGAMP-induced phosphorylation of TBK1, IRF3, and P65 was similar between *Listerin*^{fl/fl} *Lyz2-Cre* and *Listerin*^{fl/fl} macrophages (Fig. 1 K and L). Moreover, the activation of TBK1, IRF3, and P65 was attenuated by Listerin overexpression in MEF cells after HSV-1 infection (Fig. 1 M and N). Together, these results suggest that Listerin negatively regulates the cGAS–STING signaling.

Listerin Targets cGAS and Decreases Its Protein Level. Due to its ability to inhibit type I IFNs expression induced by cytoplasmic DNA but not cGAMP, we reasoned that Listerin functions at the cGAS level, upstream of cGAMP release. To confirm that Listerin targets cGAS, we conducted confocal microscopy experiments and observed the colocalization of Listerin with cGAS (Fig. 2 A and B). The in vitro pull-down assay utilizing recombinant proteins has demonstrated a conclusive association between Listerin and cGAS (Fig. 2C). Additionally, the endogenous interaction between Listerin and cGAS was detected, and the interaction was upregulated in macrophages with ISD stimulation (Fig. 2D).

Given the negative function of Listerin in the cGAS–STING pathway and the interaction between Listerin and cGAS, we further examined the effect of Listerin on the expression of cGAS protein. Our results showed that the expression of cGAS protein was elevated in *Listerin*-deficient macrophages after HSV-1 infection compared to wild-type macrophages, while, the protein levels of STING, TBK1, and IRF3 remained unaffected (Fig. 2E). Next, we found that the protein levels of cGAS were impaired in a dose-dependent manner by Listerin overexpression, while STING, TBK1, and IRF3 protein levels did not alter after Listerin overexpression (Fig. 2F). Consistent with the data that Listerin negatively regulates cGAS protein, we found that HSV-1 infection or ISD stimulation induced cGAMP synthesis was higher in Listerin-

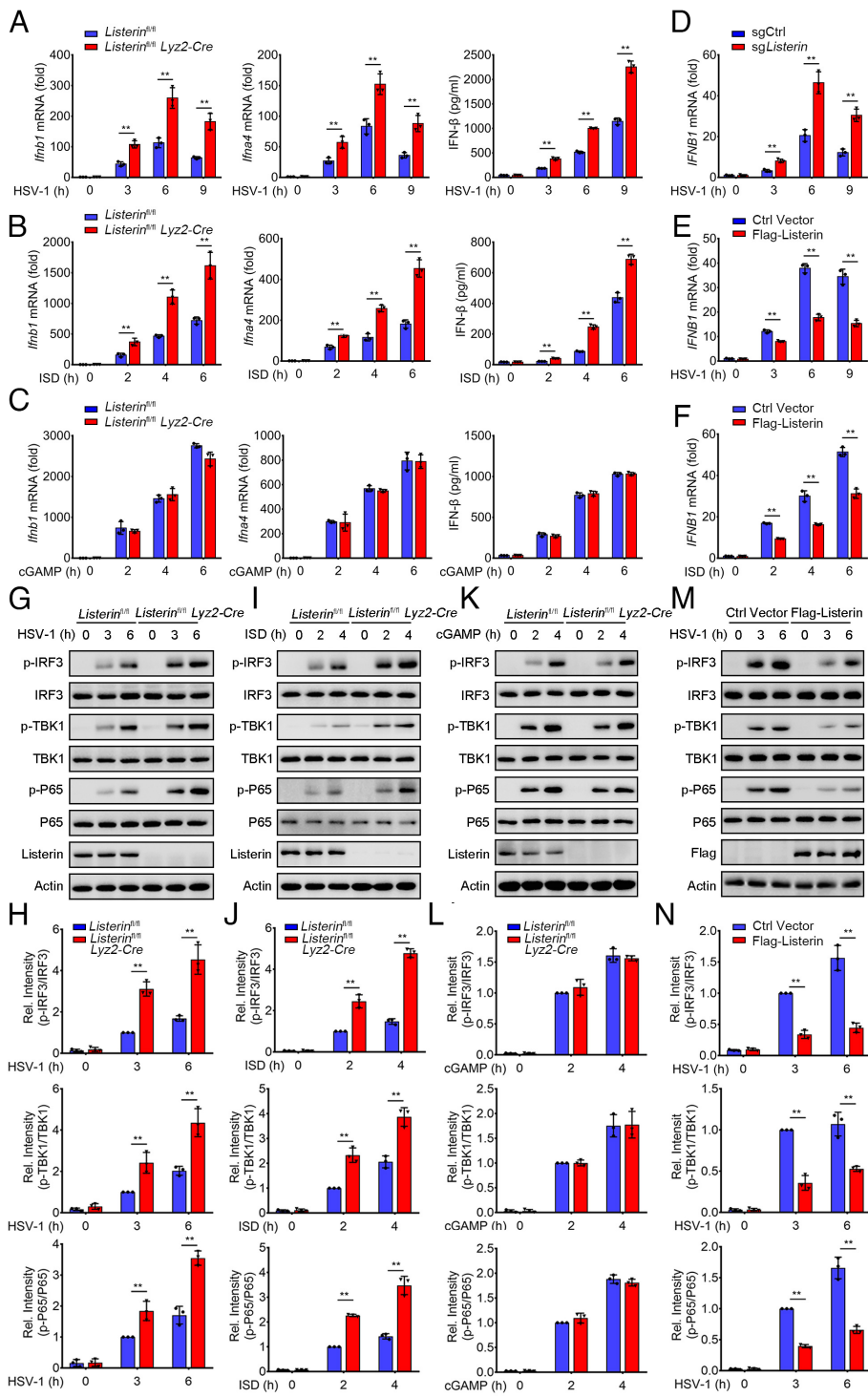


Fig. 1. Listerin deficiency promotes the cGAS-STING pathway. (A) qRT-PCR assay of *Ifnb1* and *Ifna4* mRNA and ELISA of IFN- β level in the macrophages from *Listerin*^{fl/fl} *Lyz2-Cre* and *Listerin*^{fl/fl} mice after infection by HSV-1. (B) qRT-PCR assay of *Ifnb1* and *Ifna4* mRNA and ELISA of IFN- β level in the macrophages from *Listerin*^{fl/fl} *Lyz2-Cre* and *Listerin*^{fl/fl} mice after stimulation by ISD. (C) qRT-PCR assay of *Ifnb1* and *Ifna4* mRNA and ELISA of IFN- β level in the macrophages from *Listerin*^{fl/fl} *Lyz2-Cre* and *Listerin*^{fl/fl} mice after stimulation by cGAMP. (D) qRT-PCR assay of *IFNB1* mRNA in the wild-type HeLa cells (sgCtrl) and Listerin-knockout HeLa cells (sgListerin). (E) qRT-PCR assay of *IFNB1* mRNA in the HeLa cells transfected with Ctrl Vector or Flag-Listerin after infection by HSV-1. (F) qRT-PCR assay of *IFNB1* mRNA in the HeLa cells transfected with Ctrl Vector or Flag-Listerin after stimulation by ISD. (G) Immunoblot analysis of inflammatory signaling pathways related to type I IFN and NF- κ B in macrophages from *Listerin*^{fl/fl} *Lyz2-Cre* and *Listerin*^{fl/fl} mice after infection by HSV-1. (H) Densitometric analysis of protein expression levels in G. (I) Immunoblot analysis of inflammatory signaling pathways related to type I IFN and NF- κ B in macrophages from *Listerin*^{fl/fl} *Lyz2-Cre* and *Listerin*^{fl/fl} mice after stimulation by ISD. (J) Densitometric analysis of protein expression levels in I. (K) Immunoblot analysis of inflammatory signaling pathways related to type I IFN and NF- κ B in macrophages from *Listerin*^{fl/fl} *Lyz2-Cre* and *Listerin*^{fl/fl} mice after stimulation by cGAMP. (L) Densitometric analysis of protein expression levels in K. (M) Immunoblot analysis of inflammatory signaling pathways related to type I IFN and NF- κ B in MEFs transfected with Ctrl Vector or Flag-Listerin after infection by HSV-1. (N) Densitometric analysis of protein expression levels in M. Data are representative of at least three independent experiments. Two-tailed unpaired Student's *t* test was performed with the data in A-F, H, J, L, and N; the mean \pm SD; ***P* < 0.01.

deficient macrophages (Fig. 2G). Previous related studies have demonstrated that cGAS undergoes oligomerization upon recognition of cytoplasmic DNA, which is a key step in activating cGAS and generating cGAMP (25, 26). We found that the HSV-1-induced oligomerization of cGAS was substantially elevated by knockout of Listerin in macrophages (Fig. 2H). Together, these findings suggest that Listerin decreases cGAS protein expression to regulate cGAS-STING signaling.

Listerin Promotes the Degradation of cGAS through the ESCRT Pathway. To explore the specific mechanism by which Listerin reduces cGAS protein expression, we examined the rate of cGAS

protein degradation by determining half-lives of specific proteins. Wild-type and Listerin knockout macrophages were first stimulated with ISD for 4 h and then treated with cycloheximide (CHX) for various times. Listerin deficiency significantly slowed down the degradation of cGAS both at steady and active state, but not STING, IRF3, and TBK1 (Fig. 3A and B and SI Appendix, Fig. S2A and B). These data suggest that Listerin decreases the protein level of cGAS by promoting the degradation of cGAS protein. We then investigated the degradation pathway of cGAS mediated by Listerin and found that Listerin-induced cGAS degradation could be reversed by late endosome/lysosome inhibitor bafilomycin A1, but not by proteasome inhibitor MG132 (Fig. 3C), indicating

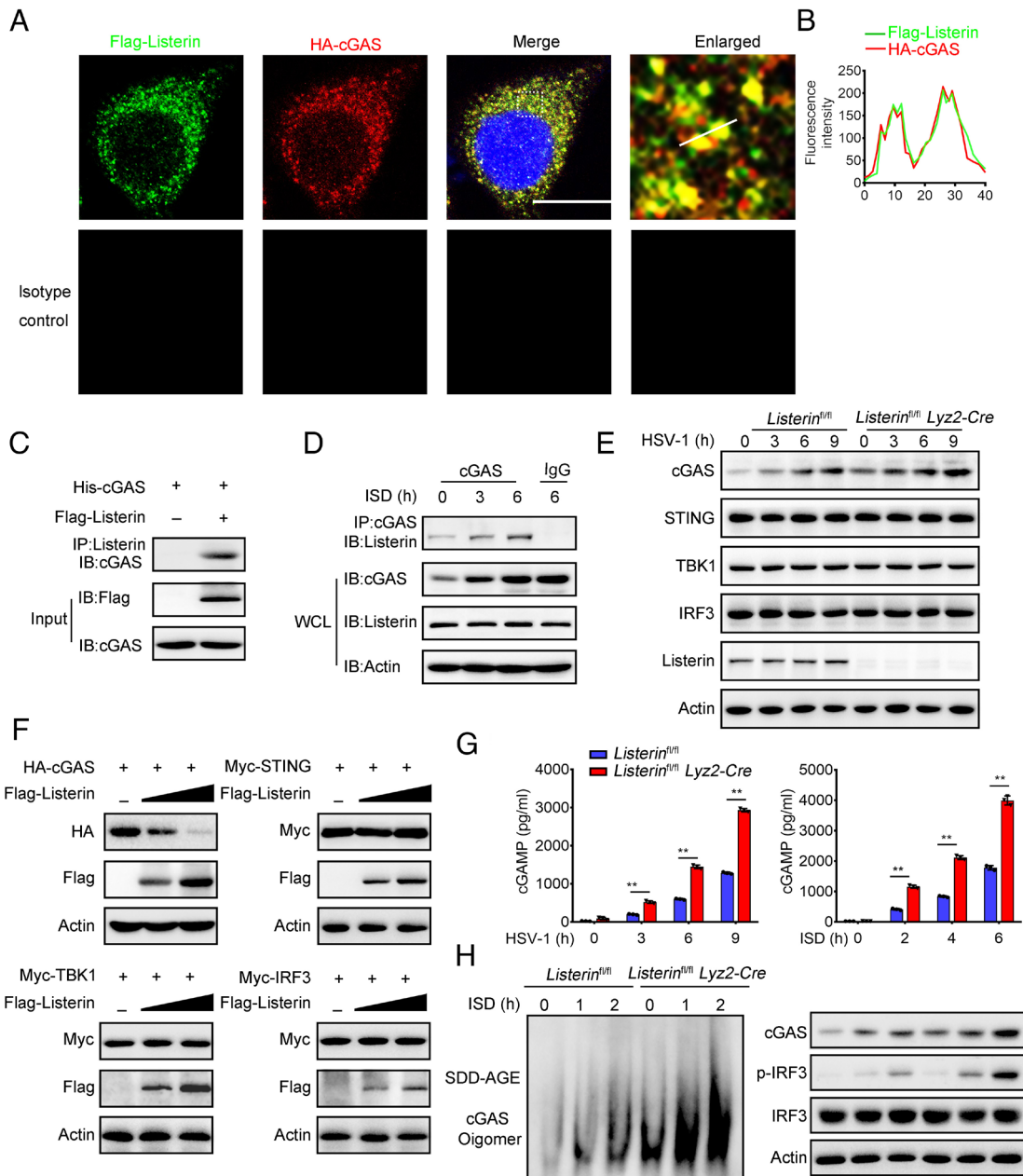


Fig. 2. Listerin targets cGAS and decreases its protein levels. (A and B) Immunostaining and fluorescence intensity analysis for Flag-Listerin and HA-cGAS in HEK293T cells. Red, HA-cGAS; green, Flag-Listerin; blue, nuclei. (Scale bar, 20 μ m.) (C) In vitro pull-down assay of cGAS with Listerin using purified recombinant proteins. (D) Immunoprecipitation and immunoblot analysis of Listerin and cGAS stimulated with ISD in mouse peritoneal macrophages for 0, 3, and 6 h. (E) Immunoblot analysis of innate signaling proteins in the macrophages from *Listerin^{fl/fl} Lyz2-Cre* and *Listerin^{fl/fl}* mice after infection by HSV-1. (F) HA-cGAS, Myc-STING, Myc-TBK1, or Myc-IRF3 were transfected into HEK293T cells together with gradient amount of Flag-Listerin, the protein levels of cGAS, STING, TBK1, or IRF3 were detected by immunoblot. (G) ELISA of the 2',3'-cGAMP level in the macrophages from *Listerin^{fl/fl} Lyz2-Cre* and *Listerin^{fl/fl}* mice after infection by HSV-1 or stimulation with ISD. (H) SDD-AGE analysis of aggregation of exogenous cGAS in the macrophages from *Listerin^{fl/fl} Lyz2-Cre* and *Listerin^{fl/fl}* mice after stimulation by ISD. Data are representative of at least three independent experiments. Two-tailed unpaired Student's *t* test was performed with the data in G; the mean \pm SD; ***P* < 0.01.

that Listerin may promote the degradation of cGAS through the autophagy/lysosome system. Some linker proteins are crucial in regulating autophagy pathways, such as Beclin1, ATG5, ATG7, and P62, which are essential for typical autophagy pathways (27–29). Taking that into consideration, we used the CRISPR/Cas9 system to generate *ATG5*- and *ATG7*-knockout HEK293T cells. Our experimental results showed that the degradation of cGAS proteins was not altered upon the knockout of *ATG5* and *ATG7* (SI Appendix, Fig. S2 C and D). We further examined the involvement of selective and chaperone-mediated autophagy in Listerin-mediated degradation by employing knockout cells for *P62* and *NDP52* and found that Listerin could still promote the

cGAS degradation in *P62*- or *NDP52*-knockout cells (SI Appendix, Fig. S2 E and F). LAMP2 plays an essential role in the process of autophagy by facilitating autophagosome formation, promoting autophagosome/lysosome fusion, and maintaining lysosomal membrane integrity (30, 31). Our results showed that Listerin was still able to promote cGAS degradation in HEK293T cells after LAMP2 knockdown using small interfering RNA (SI Appendix, Fig. S2G). These data suggest that Listerin promotes cGAS degradation independent of the classical autophagy pathway.

The ESCRT system can capture ubiquitinated proteins and subsequently sequester them into MVBs for protein degradation. ESCRT-0 is composed of HRS and STAM, which are essential

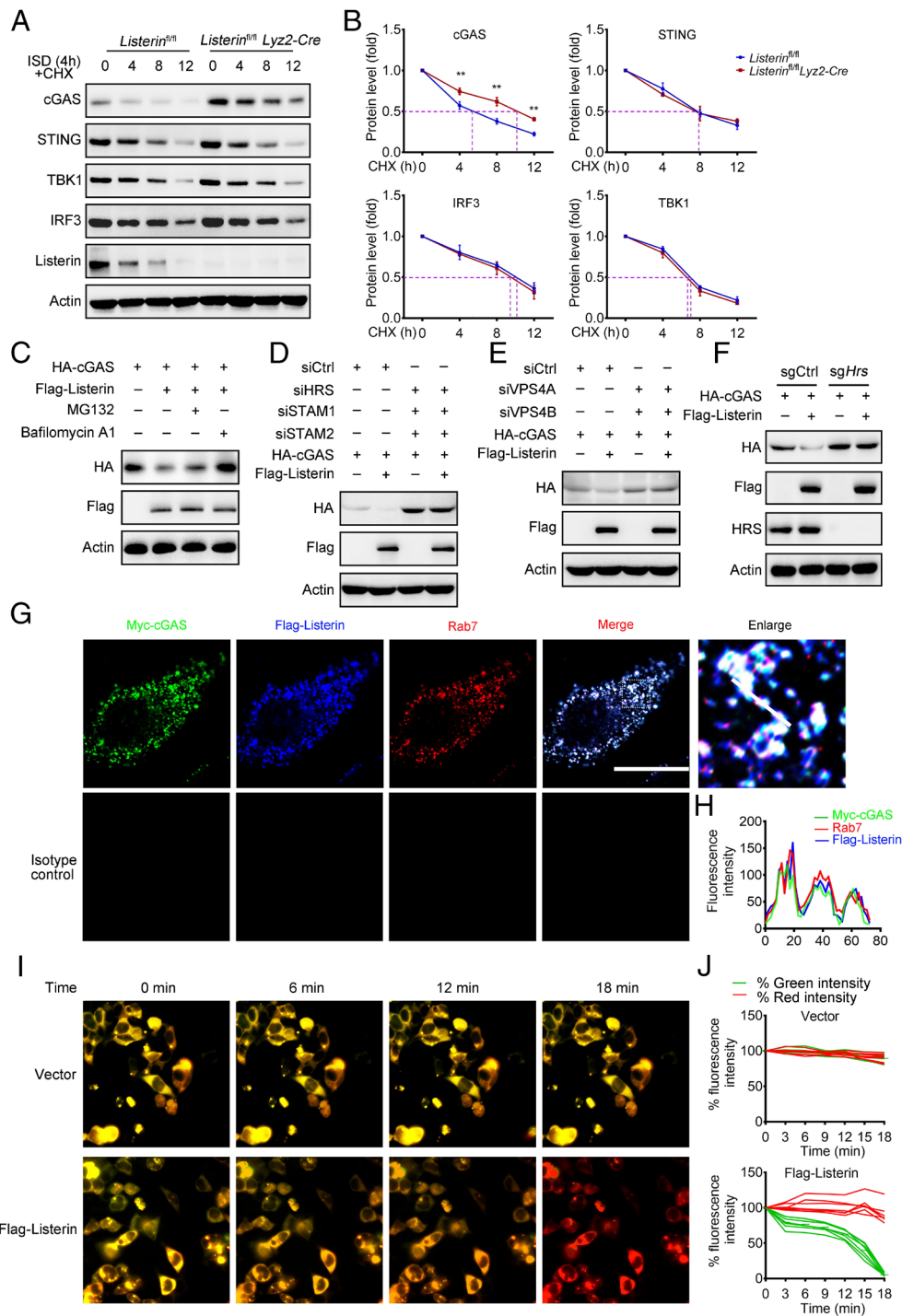


Fig. 3. Listerin promotes degradation of cGAS through the ESCRT pathway. (A) Immunoblot analysis of innate signaling proteins in *Listerin^{fl/fl}* and *Listerin^{fl/fl} Lyz2-Cre* peritoneal macrophages transfected with ISD for 4 h, and then treated with the protein synthesis inhibitor CHX for the indicated times. (B) Quantification analysis of protein degradation kinetics in A. (C) Immunoblot analysis of cGAS degradation in HEK293T cells together with Flag-Listerin followed by treated with MG132 (10 mM) or Bafilomycin A1 (0.5 μ M) for 10 h. (D) HEK293T cells were transfected with siRNA mixture against HRS, STAM1 and STAM2 or control siRNA for 24 h; then HA-cGAS and Flag-Listerin were transfected, and the levels of cGAS were detected by immunoblot analysis. (E) HEK293T cells were transfected with siRNA mixture against VPS4A and VPS4B or control siRNA for 24 h; then, HA-cGAS and Flag-Listerin were transfected, and the levels of cGAS were detected by immunoblot analysis. (F) HA-cGAS was transfected into wild-type (sgCtrl) and *Hrs*-knockout HEK293T cells (sgHrs) together with gradient amount of Flag-Listerin, the protein level of cGAS was detected by immunoblot. (G and H) Immunofluorescence analysis of HEK293T cells transfected with Myc-cGAS and Flag-Listerin. Myc-, Flag-specific immunostaining with anti-Rab7 antibody were determined by confocal microscopy analysis. (Scale bars, 20 μ m.) (I and J) GFP-mCherry-cGAS was transfected into HEK293T cells together with Listerin plasmid or control plasmid. Representative confocal time-lapse images every 6 min and quantitation of green and red fluorescence for cGAS expression. Data are representative of at least three independent experiments. ANOVA was performed with the data in B; the mean \pm SD; ** $P < 0.01$.

for the sorting of ubiquitinated cargos into endosomes. Therefore, we investigated whether the ESCRT system contributes to cGAS degradation (32). We first used a siRNA mixture simultaneously against HRS, STAM1, and STAM2 to disturb the ESCRT-0 in

HEK293T cells. Our results showed that Listerin-mediated cGAS degradation was blocked in HEK293T cells after siRNA knock-down of the ESCRT-0 subunits (Fig. 3D). Subsequently, we knocked down VPS4, which plays a crucial role in the disassembly

and release of the ESCRT-III subunit back into the cytoplasm for recycling and reuse, and found that the cGAS protein was no longer degraded by Listerin (Fig. 3E). Then, we generated the *Hrs*-knockout cell line and observed that the function of Listerin in accelerating the degradation of cGAS was completely eliminated in *Hrs*-deficient HEK293T cells (Fig. 3F). To investigate the role of ESCRT in cGAS–STING signaling, we created the small interfering RNA (siRNA) to silence for the mouse *Hrs* gene and performed the knockdown assays in peritoneal macrophages. We observed that *Ifnb1* and *Ifna4* mRNA expression was upregulated in the HRS-knockdown group compared to the control siRNA group upon HSV-1 infection or ISD transfection (SI Appendix, Fig. S2 H and I). The IFN- β secretion induced by infection with HSV-1 or stimulation with ISD was also enhanced following knockdown of HRS in macrophages (SI Appendix, Fig. S2 H and I). Moreover, ISD-induced oligomerization of cGAS was elevated by knockdown of HRS in macrophages (SI Appendix, Fig. S2J). Altogether, these data suggested that knockdown of components in ESCRT pathway enhanced cGAS activation, which further demonstrates the importance of the ESCRT pathway to cGAS regulation.

The ESCRT machinery acts at the endosome to facilitate the sorting of ubiquitinated cargo proteins (33). We found that Listerin was widely distributed on the endosomes by confocal microscopy (Fig. 3 G and H). To obtain direct evidence for the internalization of cGAS by Listerin into acidic MVB, we constructed an expression vector of GFP-mCherry-cGAS. GFP and mCherry are both fluorescent in a neutral environment, whereas the GFP signal is quenched in an acidic environment, and the mCherry signal remains stable and detectable. By time-lapse confocal imaging, we observed decreased green fluorescence intensity for cGAS in HEK293T cells transfected with Listerin with a little decrease in red fluorescence, revealing that cGAS was trafficked into acidic endosomes (Fig. 3 I and J). Taken together, these data suggest that Listerin-mediated cGAS degradation is dependent on the ESCRT machinery in endosomes.

Listerin Enhances the K63-Polyubiquitination of cGAS by Recruiting the E3 Ubiquitin Ligase TRIM27. Ubiquitination is a key signal for sorting proteins into MVBs and Listerin is an E3 ubiquitination ligase that mediates protein ubiquitination (24, 34). Therefore, we investigated whether ubiquitination of cGAS is related to the Listerin-mediated degradation. Our results showed that the endogenous ubiquitination level of cGAS was substantially reduced in *Listerin*^{fl/fl} *Lyz2-Cre* macrophages compared to that in *Listerin*^{fl/fl} macrophages after HSV-1 infection (Fig. 4A). Next, we investigate the form of cGAS linking polyubiquitin chains. WT (wild-type) HA-Ubiquitin and its mutants K48- and K63-, which have only one lysine residue at position 48 and 63 of ubiquitin, were cotransfected into HEK293T cells respectively and we found that Listerin significantly increased cGAS ubiquitination in the presence of WT and K63-Ubiquitin (Fig. 4B). Unexpectedly, the ubiquitination of cGAS induced by Listerin (ΔR), which was deprived of the RING domain, remained unchanged, suggesting that Listerin regulates the polyubiquitination of cGAS independently of its E3 enzyme activity (Fig. 4C). Therefore, we concluded that Listerin could recruit other E3 ligases to promote the polyubiquitination of cGAS with K63 polyubiquitination. After performing a mass spectrometry analysis of proteins that interact with Listerin, we have identified TRIM27, an E3 ubiquitin ligase, as a prospective binding protein of Listerin (SI Appendix, Table S2). A prior investigation has documented that TRIM27 is situated on endosomes (35). We hypothesized that Listerin may recruit TRIM27 to facilitate the degradation of cGAS. Our confocal

microscopy analysis helped us identify a strong colocalization of cGAS with both Listerin and TRIM27 (Fig. 4 D and E), as well as an extensive colocalization of Listerin and TRIM27 on the endosomes (Fig. 4 F and G). In vitro protein interaction experiments showed direct binding between cGAS and Listerin, while TRIM27 bound to cGAS only in the presence of Listerin (Fig. 4H). The in vitro ubiquitination assay demonstrated that Listerin catalyzed the K63-polyubiquitination of cGAS in the presence of TRIM27 (Fig. 4I). Finally, we verified the role of TRIM27 in the Listerin-mediated ubiquitination and degradation of cGAS. The knockdown of TRIM27 using interference RNA in HEK293T cells prevented Listerin-mediated cGAS ubiquitination and protein degradation (Fig. 4 J and K). Additionally, the knockdown of TRIM27 in Listerin-deficient peritoneal macrophages failed to increase the level of HSV-1-induced *Ifnb1* mRNA, not cGAMP (Fig. 4 L and M). Together, our data suggest that Listerin recruits the E3 ubiquitin ligase TRIM27 to promote K63-polyubiquitination and degradation of cGAS.

The HEAT Domain Is Essential for the Listerin-Mediated Degradation of cGAS. Listerin is a protein ranging from approximately 150 to 180 kilodaltons (kDa) in size and possesses a C-terminal E3-catalytic RING domain and an N-terminal domain (NTD) that are separated by a less conserved HEAT repeat domain of around 85 kDa in size (36). To identify the functional domain of Listerin that contributes to the degradation of cGAS, we constructed plasmids encoding full-length or truncated Listerin, as shown in (SI Appendix, Fig. S3A). We transfected these truncations into HeLa cells and found that Listerin (C/A) and Listerin (ΔR), which lack the E3 ubiquitin ligase function, still inhibited viral infection-induced *IFNB1* transcription. In contrast, Listerin (Δ HEAT), a mutant lacking the HEAT domain, lost its ability to inhibit *IFNB1* transcription mediated by HSV-1 infection (SI Appendix, Fig. S3B). We also noticed that Listerin mutants containing only the HEAT domain could reduce virus-induced *IFNB1* transcription (SI Appendix, Fig. S3B). In addition, we found that Listerin (Δ HEAT) was not able to promote the polyubiquitylation of cGAS (SI Appendix, Fig. S3C). Our findings suggested that the HEAT domain played an essential role in the Listerin-mediated degradation of cGAS. Next, we assessed the subcellular location of full-length and Listerin (Δ HEAT) and found that Listerin (Δ HEAT) no longer localized with Rab7 in the endosomes compared to the full-length Listerin (SI Appendix, Fig. S3 D and E). In vitro pull-down assay showed that Listerin lacking the HEAT domain attenuated the binding of TRIM27 to cGAS (SI Appendix, Fig. S3F). The data strongly indicate that the HEAT domain plays a crucial role in both the subcellular localization of Listerin within endosomes and the recruitment of TRIM27 for the ubiquitination of cGAS. We further verified the importance of the HEAT domain by transfecting Listerin (Δ HEAT) into *Listerin*-knockout HeLa cells followed by HSV-1 infection. Compared to full-length Listerin, the deletion of the HEAT domain blocked the decrease of *IFNB1* mRNA transcription induced by HSV-1 infection in *Listerin*-knockout HeLa cells (SI Appendix, Fig. S3G). Listerin (Δ HEAT) also failed to reduce the degradation of cGAS protein (SI Appendix, Fig. S3H). Furthermore, the reintroduction of full-length Listerin, but not Listerin (Δ HEAT), attenuated the HSV-1-induced phosphorylation of IRF3 or TBK1 (SI Appendix, Fig. S3I). Complementarily, we observed that the protein level of cGAS was also no longer regulated by Listerin (Δ HEAT) (SI Appendix, Fig. S3J). Together, these results suggest that the HEAT domain of Listerin plays a crucial role in regulating the degradation of cGAS.

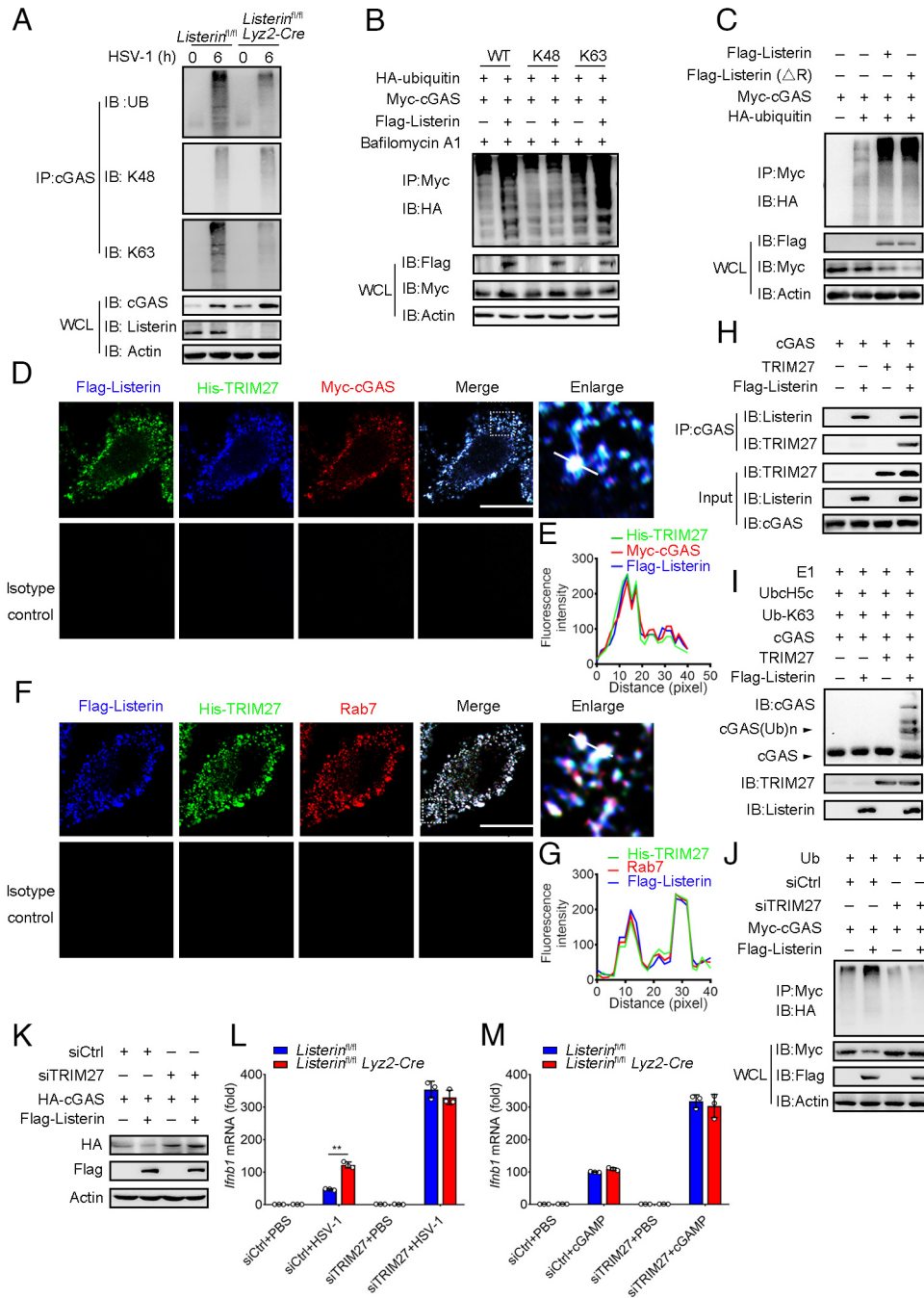


Fig. 4. Listerin enhances the K63-polyubiquitination of cGAS by recruiting the E3 ubiquitin ligase TRIM27. (A) The immunoprecipitation analysis of the ubiquitination of endogenous cGAS in macrophages from *Listerin^{fl/fl} Lyz2-Cre* and *Listerin^{fl/fl}* mice after infection with HSV-1. (B) Coimmunoprecipitation analysis of the ubiquitination of cGAS in HEK293T cells cotransfected with Myc-cGAS and HA-Ubiquitin (WT), HA-Ubiquitin-K48 or HA-Ubiquitin-K63 plasmids and Flag-Listerin followed by treatment with Bafilomycin A1. (C) Coimmunoprecipitation analysis of the ubiquitination of cGAS in HEK293T cells transfected with plasmids encoding Myc-cGAS and HA-Ubiquitin (WT), as well as a control vector or plasmids encoding Flag-Listerin, Flag-Listerin (Δ R). (D and E) Flag-, Myc-, and His-specific immunostaining of HEK293T cells transfected with His-TRIM27, Flag-Listerin, and Myc-cGAS. (Scale bars, 20 μ m.) (F and G) His-TRIM27 was transfected with Flag-Listerin into HEK293T cells, His-, Flag-specific immunostaining with anti-Rab7 antibody of HEK293T cells were determined by confocal microscopy analysis. (Scale bars, 20 μ m.) (H) In vitro pull-down assay of cGAS with Listerin, TRIM27 using purified recombinant proteins. (I) In vitro ubiquitination assay of cGAS with recombinant Listerin, TRIM27 proteins. (J) Coimmunoprecipitation analysis of the ubiquitination of cGAS in HEK293T cells transfected with siRNA-Control (siCtrl) or specific-targeting siRNA (siTRIM27) for 24 h followed by transfection of the plasmids expressing Myc-cGAS, HA-Ubiquitin, and Flag-Listerin or Flag control vector. (K) HEK293T cells were transfected with siRNA-Control (siCtrl) or specific-targeting siRNA (siTRIM27) for 24 h, then HA-cGAS and Flag-Listerin were transfected, the levels of cGAS were detected by immunoblot analysis. (L and M) qRT-PCR assay of *Ifnb1* mRNA in *Listerin^{fl/fl}* and *Listerin^{fl/fl} Lyz2-Cre* peritoneal macrophages transfected with TRIM27 transfected with siRNA-Control (siCtrl) or specific-targeting siRNA (siTRIM27) for 48 h, followed infection with HSV-1 for 6 h or stimulation with cGAMP for 4 h. Data are representative of at least three independent experiments. Two-tailed unpaired Student's t test was performed with the data in L and M; the mean \pm SD; ** $P < 0.01$.

Listerin Is Crucial for Anti-DNA Viral Innate Responses. The cGAS-STING pathway acts as a potent immune response against DNA viruses, promoting the production of IFNs and other inflammatory factors to limit viral replication and spread (37).

We investigated the antiviral function of Listerin during HSV-1 virus infection. The secretion of IFN- β was higher in *Listerin^{fl/fl} Lyz2-Cre* macrophages than in *Listerin^{fl/fl}* macrophages after the HSV-1 infection. Moreover, HSV-1 gDNA expression and HSV-1

titers were significantly attenuated in *Listerin*-deficient macrophages (Fig. 5A). We also conducted overexpression experiments to examine the role of *Listerin* in antiviral innate immunity. Notably, the overexpression of *Listerin* significantly decreased the secretion of IFN- β in MEFs following HSV-1 infection (Fig. 5B). The cGAS–STING pathway is known to induce IFN- β production as a defense against viral infection. In line with this, the overexpression of *Listerin* led to increased viral loads in MEFs (Fig. 5B). Additionally, fluorescence microscopy and flow cytometry analysis revealed higher fluorescence intensity and a greater rate of GFP-HSV-1 infected cells after overexpressing *Listerin* compared to control vector in HeLa cells (Fig. 5C and D).

To investigate the role of *Listerin* in vivo, we challenged the mice with HSV-1 virus. We observed that *Listerin*-deficient group mice exhibited elevated levels of IFN- β , TNF- α , and IL-6 in their serum compared to the control group (Fig. 5E). Moreover, we detected reduced HSV-1 gDNA expression in the brain, spleen, and lung of the *Listerin*^{fl/fl} *Lyz2-Cre* mice (Fig. 5F). Immunohistochemistry indicated that knockout of *Listerin* significantly

reduced the HSV-1 virions in the brain compared to wild-type mice (Fig. 5G and H). The plaque assay for HSV-1 titers showed that the HSV-1 replication was strikingly alleviated in the brain, spleen, and lung in the *Listerin*^{fl/fl} *Lyz2-Cre* mice than that in *Listerin*^{fl/fl} mice (Fig. 5I). In addition, *Listerin*^{fl/fl} *Lyz2-Cre* mice were observed to be more tolerant to HSV-1 infection than *Listerin*^{fl/fl} mice (Fig. 5J). Overall, these data demonstrate that *Listerin* deficiency enhances the anti-DNA viral innate responses.

Genetic Deletion of *Listerin* Deteriorates the Neuroinflammation in an ALS Mice Model. In addition to DNA viruses, mtDNA entering cytoplasm in large quantities can also activate cGAS to induce IFN-I production. TDP-43 protein accumulation has been observed in neurons of nearly all patients with sporadic ALS (38). It has been reported that the invasion of the TDP-43 protein leads to the release of mtDNA from mitochondria, activating cGAS and initiating neuroinflammation to aggravate the progression of ALS disease (9). We then evaluated whether the regulation of *Listerin* on cGAS affects the disease course of ALS.

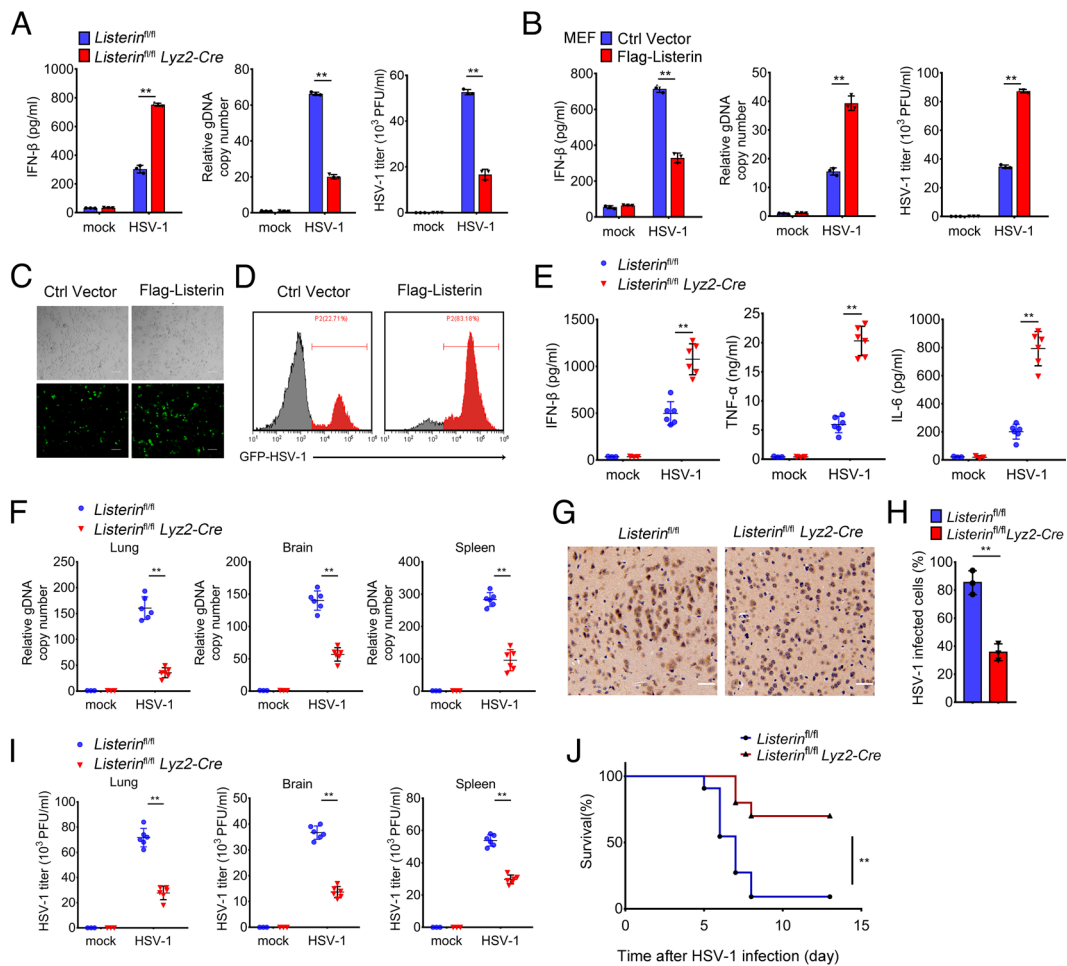


Fig. 5. *Listerin* is crucial for anti-DNA viral innate responses. (A) Secretion of IFN- β measured by ELISA, HSV-1 gDNA measured by qPCR or HSV-1 titers measured by the plaque assay in macrophages from *Listerin*^{fl/fl} and *Listerin*^{fl/fl} *Lyz2-Cre* mice infected with HSV-1 for 12 h. (B) Secretion of IFN- β measured by ELISA, HSV-1 gDNA measured by qPCR or HSV-1 titers measured by the plaque assay in MEFs transfected with Flag-*Listerin* and control plasmid (Ctrl Vector) followed by infection with HSV-1 for 12 h. (C and D) HeLa cells were transfected with Flag-*Listerin* and control plasmid (Ctrl Vector) followed by infection with GFP-HSV-1 for 12 h; GFP-HSV-1 replication was determined by fluorescence microscopy (bright-field, upper; fluorescence, bottom). Scale bars, 100 μ m) and quantification of fluorescence intensity using flow cytometry. (E) IFN- β , TNF- α , and IL-6 secretion in sera from *Listerin*^{fl/fl} and *Listerin*^{fl/fl} *Lyz2-Cre* mice after intraperitoneal injection for 8 h with HSV-1 (5×10^7 PFU per mouse). (F) Expression of HSV-1 gDNA in the lung, brain, and spleen by qPCR analysis from *Listerin*^{fl/fl} and *Listerin*^{fl/fl} *Lyz2-Cre* mice infected for 48 h by intraperitoneal injection of HSV-1 for 48 h (5×10^7 PFU per mouse). (G and H) HSV-1-specific immunohistochemistry analysis of brain from *Listerin*^{fl/fl} and *Listerin*^{fl/fl} *Lyz2-Cre* mice infected for 48 h by intraperitoneal injection of HSV-1 for 48 h (5×10^7 PFU per mouse). (Scale bars, 40 μ m). (I) HSV-1 titers analysis in the lung, brain, and spleen by qPCR analysis from *Listerin*^{fl/fl} and *Listerin*^{fl/fl} *Lyz2-Cre* mice infected for 48 h by intraperitoneal injection of HSV-1 for 48 h (5×10^7 PFU per mouse). (J) Survival of *Listerin*^{fl/fl} and *Listerin*^{fl/fl} *Lyz2-Cre* mice after intravenous injection of HSV-1 (1×10^8 PFU per mouse). Data are representative of at least three independent experiments. Two-tailed unpaired Student's *t* test was performed with the data in A, B, E, F, H, and I; the mean \pm SD; the log-rank Mantel-Cox test was used in J. ***P* < 0.01.

Accumulating studies have shown that microglia can release inflammatory cytokines, which can damage the structure and function of neurons and ultimately lead to neuronal degeneration and death (39, 40). We generated *Listerin*-conditional knockout mice specifically in microglia by crossing *Listerin*^{fl/fl} with microglia-specific *Cx3cr1-cre* mice (*Listerin*^{fl/fl} *Cx3cr1-Cre*). Primary microglia from *Listerin*^{fl/fl} *Cx3cr1-Cre* mice showed obvious upregulation of *Ifnb1*, *Tnfa*, *Il6*, and *Il12b* mRNA upon stimulating with TDP-43 protein compared to microglia from *Listerin*^{fl/fl} mice (SI Appendix, Fig. S4A). ELISA also detected higher cytokine secretion of IFN- β , TNF- α , IL-6, and IL-12p40 in *Listerin*-deficient primary microglia (Fig. 6A). We also observed similar findings in mouse BV2 cells, in which small interfering RNA (siListerin) mediated-knockdown of *Listerin* led to augmentation of cytokine gene expression (SI Appendix, Fig. S4 B and C). Moreover, overexpression of Flag-*Listerin* in MEFs attenuated the *Ifnb1*, *Tnfa*, *Il6*, and *Il12b* mRNA induced with TDP-43 stimulation (SI Appendix, Fig. S4D). Consistently, deficiency of *Listerin* in microglia exhibited increased phosphorylation of TBK1, IRF3, and P65 upon TDP-43 stimulation (Fig. 6B). TDP-43 protein-triggered phosphorylation of TBK1, IRF3, and P65 was also enhanced in BV2 cells transfected with *Listerin* siRNA compared with a control siRNA (SI Appendix, Fig. S4E).

The TDP-43 Q331K mutation is a genetic variant that promotes the aberrant aggregation of TDP-43 in ALS (41). Indeed, we found

transfection of TDP-43 Q331K in MEFs could induce more phosphorylation of TBK1, IRF3, and P65 compared to that of WT TDP-43. While, overexpression of *Listerin* inhibited the phosphorylation of TBK1, IRF3, and P65 induced by both WT and mutant TDP-43 transfection (SI Appendix, Fig. S5A). We also noticed increased cGAS protein level in primary microglia from *Listerin*^{fl/fl} *Cx3cr1-Cre* mice compared to that from *Listerin*^{fl/fl} mice upon TDP-43 stimulation (Fig. 6C). However, overexpression of *Listerin* in MEFs greatly reduced cGAS protein level induced by WT and mutant TDP-43 transfection (SI Appendix, Fig. S5B). Therefore, we conclude that *Listerin* deletion promoted TDP-43-induced neuroinflammation by regulating the cGAS–STING pathway.

In order to assess the function of *Listerin* in microglia on the regulation of neuronal toxicity, we cocultured WT neurons with microglia in a non-contact transwell system that allowed for the exchange of soluble cytokines (Fig. 6D). We found that microglia treated with TDP-43 protein triggered neuronal cell death, as measured by Hoechst/PI (propidium iodide) staining. Intriguingly, microglia deficient of *Listerin* triggered a greater extent of neuronal cell death compared to WT microglia after stimulation with TDP-43 protein (Fig. 6 E and F). We further showed that microglia lacking *Listerin* caused more apoptosis of neuronal cells treated with TDP-43 protein, as determined by Annexin V-FITC/PI staining (SI Appendix, Fig. S5 C and D). The LDH assay revealed higher levels of LDH release from neuronal cells cocultured with

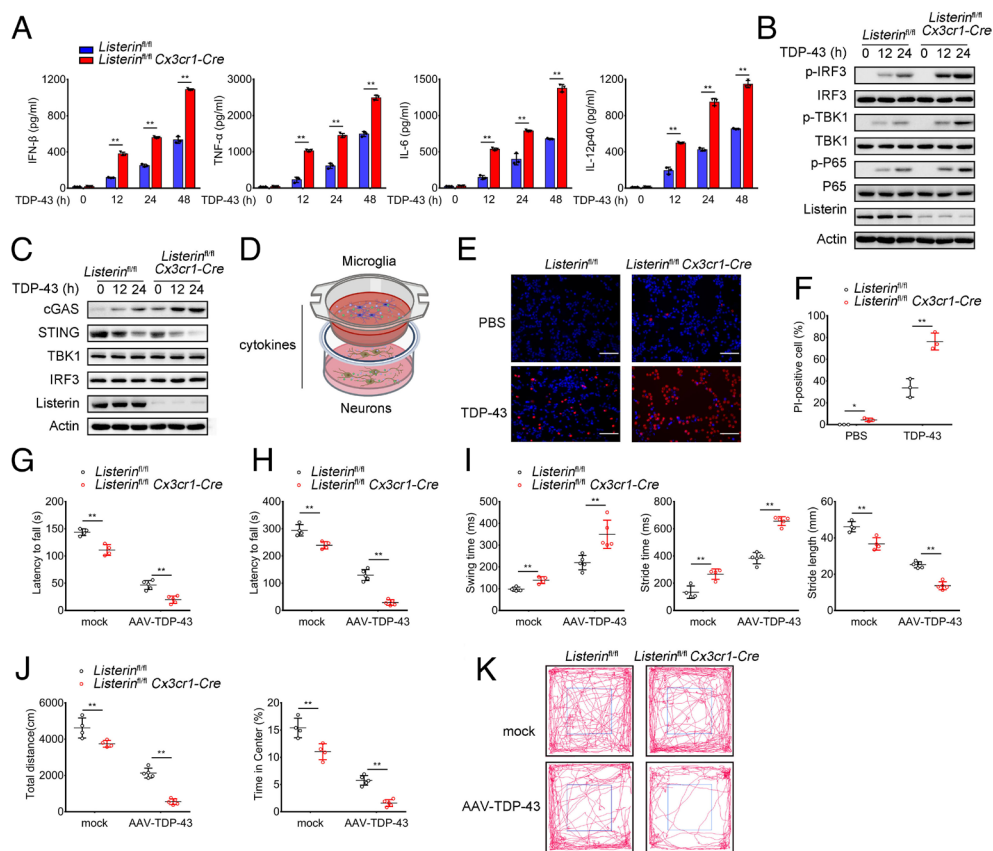


Fig. 6. Genetic deletion of *Listerin* deteriorates the neuroinflammation in ALS. (A) ELISA of IFN- β , TNF- α , IL-6, and IL-12p40 level in the microglial from *Listerin*^{fl/fl} and *Listerin*^{fl/fl} *Cx3cr1-Cre* mice after stimulation with TDP-43 protein. (B) Immunoblot analysis of inflammatory signaling pathways related to type I IFN and NF- κ B in the microglial from *Listerin*^{fl/fl} and *Listerin*^{fl/fl} *Cx3cr1-Cre* mice after stimulation with TDP-43 protein. (C) Immunoblot analysis of innate signaling proteins in the microglial from *Listerin*^{fl/fl} and *Listerin*^{fl/fl} *Cx3cr1-Cre* mice after stimulation with TDP-43 protein. (D) Schematic representation of the coculture model: Primary microglia prepared from *Listerin*^{fl/fl} and *Listerin*^{fl/fl} *Cx3cr1-Cre* mice were plated on transwells. Primary hippocampal neurons from wild-type mice were plated in 12-well plates. (E and F) Representative images and the analysis of Hoechst and propidium iodide (PI) staining from primary hippocampal neurons coincubated with primary microglia prepared from *Listerin*^{fl/fl} and *Listerin*^{fl/fl} *Cx3cr1-Cre* mice, and further incubated with TDP-43 protein for 3 d. (Scale bar, 20 μ m.) (G–K) *Listerin*^{fl/fl} and *Listerin*^{fl/fl} *Cx3cr1-Cre* mice were injected with mock or AAV-TDP-43 virus in brains, the rotarod test (G), the hanging wire test (H), the gait test (I), and open field test (J and K) were performed. Data are representative of at least three independent experiments. Two-tailed unpaired Student's t test was performed with the data in A and F–J; the mean \pm SD; * P < 0.05, ** P < 0.01.

Listerin-deficient microglia, indicating impaired neuronal function (*SI Appendix, Fig. S5E*). These findings suggest that Listerin inhibits neuroinflammation associated with ALS, consequently mitigating TDP-43-induced neurotoxicity.

We further investigated whether Listerin plays a role in the ALS mice model through injection of abnormal TDP-43 in vivo. TDP-43 adeno-associated virus (AAV) 9 expression vector (AAV-TDP-43) was constructed and injected into the striatum in the brain of *Listerin^{fl/fl}* mice and *Listerin^{fl/fl} Cx3cr1-Cre* mice by stereo localization. Compared with wild-type mice, *Listerin^{fl/fl} Cx3cr1-Cre* mice injected with the AAV-TDP-43 virus maintained a shorter maintain latency in the accelerated rotarod test, which is considered the gold standard to measure coordinated movement and balance ability (Fig. 6G). The mice *Listerin^{fl/fl} Cx3cr1-Cre* mice exhibited weaker grip function in the hanging wire test compared with wild-type mice (Fig. 6H). Meanwhile, knockout Listerin in mice aggravated the gait disorder, as showed by shorter swing time and stride time, as well as longer stride length (Fig. 6I). In further tests, *Listerin* deficient mice shortened the walking distance and decreased the fraction of time they spent in the central area in the open field test (Fig. 6J and K). These data suggested that Listerin deficiency exacerbates neurodegeneration in an ALS mouse model.

Listerin Alleviates Neurodegeneration in an ALS Mouse Model.

We next explored the potential therapeutic possibility of Listerin to slow the ALS disease progression. We synthesized an adenovirus vector overexpressing Listerin (Adv-Listerin) and used it to treat the Prp-TDP-43^{Tg/+} mice, which served as a classical ALS disease model (Fig. 7A). We found that stereotaxic injection of Adv-Listerin alleviated motor deficits in Prp-TDP-43^{Tg/+} mice through some behavioral detections. Compared with wild-type mice, Prp-TDP-43^{Tg/+} mice injected with Adv-Listerin were steadier to maintain latency in the accelerated rotarod test (Fig. 7B). In addition, the mice with adenovirus-mediated overexpression of

Listerin showed stronger grip function in the hanging wire test compared with wild-type mice (Fig. 7C). Meanwhile, Listerin-overexpression mice performed better in gait detection than wild-type mice, as showed by shorter swing time and stride time, as well as longer stride length (Fig. 7D). Moreover, we also noticed that Adv-Listerin injection extended the walking distance of ALS mice and increased the fraction of time they spent in the central area in the open field test (Fig. 7E and F). Consistently, we proved that the overexpression of Listerin in the Prp-TDP-43^{Tg/+} model leads to decreased cGAS-mediated neuroinflammation. In particular, we observed that overexpression of Listerin in mice resulted in less expression of type I interferon and inflammatory factors in the cortex, including IFN- β , TNF- α , IL-6, and IL-12p40 (Fig. 7G). We also examined the level of cGAMP in serum and cortex samples and found that the expression of cGAMP was significantly reduced in Prp-TDP-43^{Tg/+} mice after overexpression of Listerin (Fig. 7H). Additionally, we assessed that Listerin-injected mice showed slighter loss of neurons in the cortex compared to wild-type mice using NisslBody staining (Fig. 7I and J). These results suggest that Listerin plays a critical role in regulating neuroinflammation and neuronal loss and could be a potential therapeutic target for ALS-related neurodegenerative disorders.

Discussion

cGAS is a crucial cytoplasmic DNA sensor that plays a vital role in the innate immune response (7, 42). However, its excessive or dysregulated activation may lead to the infectious, autoimmune, neoplastic, and neurodegenerative disorders that can have long term effects on human health. Thus, the timely degradation of cGAS is essential to maintain cell homeostasis. Ubiquitination plays a crucial role in the degradation of cGAS, which serves as a negative regulatory mechanism for the cGAS signaling pathway. For instance, HSP27 facilitates the ubiquitination of cGAS,

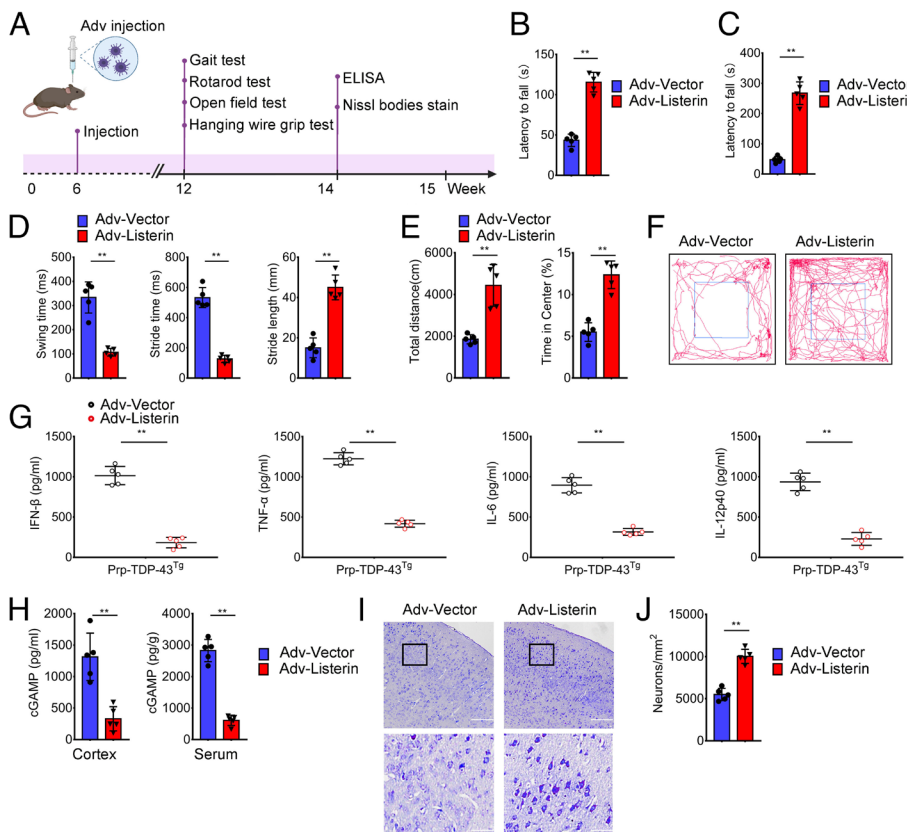


Fig. 7. Listerin alleviates neurodegeneration in an ALS mouse model. (A) Schematic diagram of the animal experimental design. (B–F) Prp-TDP-43^{Tg/+} mice were injected with Adv-Vector or Adv-Listerin virus in brains as in A, the rotarod test (B), the hanging wire test (C), the gait test (D), and open field test (E and F) were performed. (G) ELISA of IFN- β , TNF- α , IL-6, and IL-12p40 levels in the brains of Prp-TDP-43^{Tg/+} mice treated as in A. (I and J) Representative Nissl body staining and analysis (cresyl violet) of a coronal section (scale bars, 100 μ m) in the brains of Prp-TDP-43^{Tg/+} mice treated as in A. Data are representative of at least three independent experiments. Two-tailed unpaired Student's *t* test was performed with the data in B–E, G, H, and J; the mean \pm SD; ***P* < 0.01.

resulting in its proteasome-dependent degradation and subsequent suppression of the cGAS-mediated interferon signaling (43). The K48-linked ubiquitination of cGAS mediates degradation of cGAS via the P62-dependent selective autophagy pathway (44). UL21 recruits the E3 ligase UBE3C to catalyze the K27-linked ubiquitination of cGAS, which is recognized by the cargo receptor toll interaction protein and degraded in the lysosomes (45). Another important pathway for ubiquitination protein degradation is the ESCRT pathway; however, there have been no reports confirming the involvement of the ESCRT pathway in the degradation of cGAS.

The E3 ubiquitin ligase Listerin (LTN1 in yeast) eliminates the aberrant nascent polypeptides through ubiquitination modification of the aberrant nascent polypeptides for the degradation on stalled ribosomes (23, 46, 47). Most of the studies about Listerin were performed in yeast and in vitro system, but there was little research on its physiological function in eukaryotes. Listerin has been linked to neurodegenerative diseases in a forward genetic screen study in mice, which reported that Listerin mutant mice are prone to develop severe motor deficits. Along with an increase of larger diameter axons, Listerin mutant mice exhibited a significant loss of large axonal fibers that are typical of ALS (48). However, the exact mechanisms of how defects in Listerin lead to specific neurodegenerative phenotypes are not known. In order to resolve a few unanswered questions, we created the Listerin-deficient mice to investigate its physiological function. We found that Listerin-deficient mice showed more severe ALS-related neurobehavioral symptoms and increased neuroinflammation, which can be alleviated by overexpression of Listerin. Another related study has revealed that TDP-43 induced the leakage of mtDNA into the cytoplasm by impairing mitochondria. cGAS detected these mtDNA and initiated the activation of the IFN and NF- κ B signaling pathways, ultimately leading to neuroinflammation and exacerbating the progression of ALS (9). In our study, we found that Listerin targets cGAS and promotes its degradation via the ESCRT pathway. This mechanism effectively alleviates the neuroinflammation triggered by cGAS activation. These findings provide further evidence supporting the therapeutic potential of targeting the cGAS–STING signaling pathway in the management of ALS.

Our research confirmed that Listerin is a promising therapeutic target for ALS. So we set up detailed experiments to further explore the regulatory mechanisms of Listerin. Listerin comprises a conserved NTD, ARM/HEAT repeats, and a RING domain in the C-terminal. The NTD is required to interact with 60S subunits, and the RING domain provides E3 ligase activity required for the ubiquitination and degradation of nascent proteins (49). However, the function of the ARM/HEAT repeats remains enigmatic, although they are assumed to solely represent the link between Listerin ends and distal sites on the ribosome (36, 50). Unexpectedly, we found that the HEAT domain of Listerin plays a crucial role in facilitating the activation of the cGAS–STING pathway. Listerin loses its ability to regulate IFN production in the absence of the HEAT domain. Moreover, our study provides evidence that the HEAT domain is essential for the endosomal localization and the recruitment of E3 ligase for Listerin, enabling the ubiquitination of cGAS and subsequent endosomal degradation. These findings underscore the importance of the HEAT domain in mediating the regulation of the cGAS–STING pathway.

The results of our investigation also indicate that the Listerin–TRIM27 axis can be employed to modulate the expression of cGAS at its basal levels. Specifically, we observed that the absence of Listerin led to an elevation in cGAS protein levels, both during periods of stability and heightened activity. (Fig. 2E). Besides, we

detected the cGAS protein half-life under steady state conditions and found the cGAS protein half-life is also longer in Listerin knockout macrophage (SI Appendix, Fig. S2A). Therefore, we think the degradation of cGAS by the Listerin–TRIM27–ESCRT pathway happens both at steady and active state. TRIM27 is an E3 ubiquitin ligase involved in regulating immune responses. It has been shown to negatively regulate the production of IFN- β by regulating the degradation of IKK/TBK1 through its E3 ubiquitin ligase activity (51, 52). We found that TRIM27 mediated the K63-linked ubiquitin modification of cGAS for degradation in an ESCRT-dependent mechanism. Our study identified a regulatory mechanism by which TRIM27 is involved in antiviral immunity by regulating cGAS, which provides insights and a broader perspective that further sheds light on TRIM27's contribution to the antiviral immune process.

Our study reveals that Listerin promotes the K63 ubiquitination of cGAS by recruiting TRIM27, resulting in the degradation of cGAS through the ESCRT pathway. Our research revealed a new mechanism for regulating cGAS degradation through the ESCRT pathway and identified that overexpression of Listerin can relieve neurobehavioral symptoms and pathological damage in ALS mice. Hence, targeting Listerin to alleviate inflammation resulting from the overactivation of the cGAS–STING signaling pathway represents a promising therapeutic strategy. Our study explores the physiological function of Listerin, which can provide insights into the functional links between Listerin and disease-related processes.

Materials and Methods

Animal studies were approved by the Scientific Investigation Board of the Medical School of Shandong University. Detailed descriptions of *Virus Strains, Cell Cultures, RNA Extraction, RT-PCR, Western Blot, Confocal Microscopy, Virus Infection In Vivo, Protein Purification, In Vitro Ubiquitination Assay, Mass Spectrometry Analysis, Stereotactic Surgery and Injection, Behavioral Test, Mouse Brain Tissue Collection, and Statistical Analysis* are provided in SI Appendix.

Data, Materials, and Software Availability. All study data are included in the article and/or SI Appendix.

ACKNOWLEDGMENTS. We kindly thank many colleagues who provided key reagents. *ATG5*-, *NDP52*-, and *P62*-knockout HEK293T cells were provided by Prof. JunCui (Sun Yat-sen University, China). iPSC was a kind gift from Dr. Huili Hu (Shandong University, China). We also thank the technical support for confocal microscopy analysis from M. L. Wu and Y. Yu in Translational Medicine Core Facility of Advanced Medical Research Institute, Shandong University. This work was supported by grants from the National Natural Science Foundation of China (82321002, 32230033, and 81930039 to C.G.; 82222027, 32270918, and 31900680 to B.L.), grants from the National key research and development program (2021YFC2300603 to C.G.), grants from Natural Science Foundation of Shandong Province (ZR201911140289 to C.G.) and the grants from Shandong Provincial Natural Science Foundation (ZR2021YQ48, ZR2018BC021, ZR2021ZD08 to B.L.).

Author affiliations: ^aDepartment of Immunology and Key Laboratory of Infection and Immunity of Shandong Province & Key Laboratory for Experimental Teratology of Ministry of Education, Shandong University, Jinan, Shandong 250012, People's Republic of China; ^bDepartment of Immunology, School of Basic Medical Sciences, Shandong University, Jinan, Shandong 250012, People's Republic of China; ^cDepartment of Pathogenic Biology, School of Basic Medical Sciences, Shandong University, Jinan, Shandong 250012, People's Republic of China; and ^dAdvanced Medical Research Institute, Cheeloo College of Medicine, Shandong University, Jinan, Shandong 250012, People's Republic of China

Author contributions: B.L. and C.G. designed research; F.Q., B.C., R.C., Y. Zhang, and B.L. performed research; T.C., F.L., W.S., Y. Zheng, X.Q., W.Z., and C.G. contributed new reagents/analytic tools; F.Q., B.C., R.C., X.B., J.Y., Y. Zhang, Y.L., B.L., and C.G. analyzed data; and F.Q., B.L., and C.G. wrote the paper.

The authors declare no competing interest.

1. S. W. Brubaker, K. S. Bonham, I. Zanoni, J. C. Kagan, Innate immune pattern recognition: A cell biological perspective. *Annu. Rev. Immunol.* **33**, 257–290 (2015).
2. Q. Chen, L. Sun, Z. J. Chen, Regulation and function of the cGAS-STING pathway of cytosolic DNA sensing. *Nat. Immunol.* **17**, 1142–1149 (2016).
3. E. L. Mills, B. Kelly, L. A. J. O'Neill, Mitochondria are the powerhouses of immunity. *Nat. Immunol.* **18**, 488–498 (2017).
4. J. Wu, Z. J. Chen, Innate immune sensing and signaling of cytosolic nucleic acids. *Annu. Rev. Immunol.* **32**, 461–488 (2014).
5. X. Zhang, X. C. Bai, Z. J. Chen, Structures and mechanisms in the cGAS-STING innate immunity pathway. *Immunity* **53**, 43–53 (2020).
6. K. P. Hopfner, V. Hornung, Molecular mechanisms and cellular functions of cGAS-STING signalling. *Nat. Rev. Mol. Cell Biol.* **21**, 501–521 (2020).
7. M. Motwani, S. Pesiridis, K. A. Fitzgerald, DNA sensing by the cGAS-STING pathway in health and disease. *Nat. Rev. Genet.* **20**, 657–674 (2019).
8. Y. Zhao, M. Simon, A. Seluanov, V. Gorbunova, DNA damage and repair in age-related inflammation. *Nat. Rev. Immunol.* **23**, 75–89 (2023).
9. C. H. Yu *et al.*, TDP-43 triggers mitochondrial DNA release via mPTP to activate cGAS/STING in ALS. *Cell* **183**, 636–649.e18 (2020).
10. Anonymous, Microglial cGAS-STING links innate immunity and Alzheimer's disease. *Nat. Aging* **3**, 155–156 (2023).
11. Y. Hou *et al.*, NAD(+) supplementation reduces neuroinflammation and cell senescence in a transgenic mouse model of Alzheimer's disease via cGAS-STING. *Proc. Natl. Acad. Sci. U.S.A.* **118**, e2011226118 (2021).
12. S. Wang *et al.*, ALDH2 contributes to melatonin-induced protection against APP/PS1 mutation-prompted cardiac anomalies through cGAS-STING-TBK1-mediated regulation of mitophagy. *Signal Transduct. Target. Ther.* **5**, 119 (2020).
13. J. T. Hinkle *et al.*, STING mediates neurodegeneration and neuroinflammation in nigrostriatal α -synucleinopathy. *Proc. Natl. Acad. Sci. U.S.A.* **119**, e2118819119 (2022).
14. N. Zheng, N. Shabek, Ubiquitin ligases: Structure, function, and regulation. *Annu. Rev. Biochem.* **86**, 129–157 (2017).
15. D. A. Cruz Walma, Z. Chen, A. N. Bullock, K. M. Yamada, Ubiquitin ligases: Guardians of mammalian development. *Nat. Rev. Mol. Cell Biol.* **23**, 350–367 (2022).
16. M. Vietri, M. Radulovic, H. Stenmark, The many functions of ESCRTs. *Nat. Rev. Mol. Cell Biol.* **21**, 25–42 (2020).
17. M. L. Skowrya, P. H. Schlesinger, T. V. Naismith, P. I. Hanson, Triggered recruitment of ESCRT machinery promotes endolysosomal repair. *Science* **360**, eaar5078 (2018).
18. J. McCullough, A. Frost, W. I. Sundquist, Structures, functions, and dynamics of ESCRT-III/Vps4 membrane remodeling and fission complexes. *Annu. Rev. Cell Dev. Biol.* **34**, 85–109 (2018).
19. M. Gentili *et al.*, ESCRT-dependent STING degradation inhibits steady-state and cGAMP-induced signalling. *Nat. Commun.* **14**, 611 (2023).
20. Y. Kuchitsu *et al.*, STING signalling is terminated through ESCRT-dependent microautophagy of vesicles originating from recycling endosomes. *Nat. Cell Biol.* **25**, 453–466 (2023).
21. K. R. Balka *et al.*, Termination of STING responses is mediated via ESCRT-dependent degradation. *EMBO J.* **42**, e112712 (2023). [10.15252/embj.2022112712](https://doi.org/10.15252/embj.2022112712).
22. A. Decout, J. D. Katz, S. Venkatraman, A. Ablasser, The cGAS-STING pathway as a therapeutic target in inflammatory diseases. *Nat. Rev. Immunol.* **21**, 548–569 (2021).
23. C. A. P. Joazeiro, Mechanisms and functions of ribosome-associated protein quality control. *Nat. Rev. Mol. Cell Biol.* **20**, 368–383 (2019).
24. M. H. Bengtson, C. A. Joazeiro, Role of a ribosome-associated E3 ubiquitin ligase in protein quality control. *Nature* **467**, 470–473 (2010).
25. W. Zhou *et al.*, Structure of the human cGAS-DNA complex reveals enhanced control of immune surveillance. *Cell* **174**, 300–311.e11 (2018).
26. Q. Yin, T. M. Fu, J. Li, H. Wu, Structural biology of innate immunity. *Annu. Rev. Immunol.* **33**, 393–416 (2015).
27. Y. Nishida *et al.*, Discovery of Atg5/Atg7-independent alternative macroautophagy. *Nature* **461**, 654–658 (2009).
28. E. Wirawan *et al.*, Beclin1: A role in membrane dynamics and beyond. *Autophagy* **8**, 6–17 (2012).
29. I. Dikic, Z. Elazar, Mechanism and medical implications of mammalian autophagy. *Nat. Rev. Mol. Cell Biol.* **19**, 349–364 (2018).
30. S. Notomi *et al.*, Genetic LAMP2 deficiency accelerates the age-associated formation of basal laminar deposits in the retina. *Proc. Natl. Acad. Sci. U.S.A.* **116**, 23724–23734 (2019).
31. P. M. Rodrigues *et al.*, LAMP2 regulates autophagy in the thymic epithelium and thymic stroma-dependent CD4T cell development. *Autophagy* **19**, 426–439 (2023).
32. T. Wollert, J. H. Hurley, Molecular mechanism of multivesicular body biogenesis by ESCRT complexes. *Nature* **464**, 864–869 (2010).
33. A. K. Pfitzner *et al.*, An ESCRT-III polymerization sequence drives membrane deformation and fission. *Cell* **182**, 1140–1155.e18 (2020).
34. R. L. Williams, S. Urbé, The emerging shape of the ESCRT machinery. *Nat. Rev. Mol. Cell Biol.* **8**, 355–368 (2007).
35. Y. H. Hao *et al.*, Regulation of WASH-dependent actin polymerization and protein trafficking by ubiquitination. *Cell* **152**, 1051–1064 (2013).
36. S. K. Doamekpor *et al.*, Structure and function of the yeast listerin (Ltn1) conserved N-terminal domain in binding to stalled 60S ribosomal subunits. *Proc. Natl. Acad. Sci. U.S.A.* **113**, E4151–E4160 (2016).
37. C. Chen, P. Xu, Cellular functions of cGAS-STING signaling. *Trends Cell Biol.* **33**, 630–648 (2022). [10.1016/j.tcb.2022.11.001](https://doi.org/10.1016/j.tcb.2022.11.001).
38. M. Neumann *et al.*, Ubiquitinated TDP-43 in frontotemporal lobar degeneration and amyotrophic lateral sclerosis. *Science* **314**, 130–133 (2006).
39. C. K. Glass, K. Saijo, B. Winner, M. C. Marchetto, F. H. Gage, Mechanisms underlying inflammation in neurodegeneration. *Cell* **140**, 918–934 (2010).
40. A. Ndoja *et al.*, Ubiquitin ligase COP1 suppresses neuroinflammation by degrading cEBP β in microglia. *Cell* **182**, 1156–1169.e12 (2020).
41. E. Kabashi *et al.*, TARDBP mutations in individuals with sporadic and familial amyotrophic lateral sclerosis. *Nat. Genet.* **40**, 572–574 (2008).
42. Z. Ma, B. Damania, The cGAS-STING defense pathway and its counteraction by viruses. *Cell Host Microbe* **19**, 150–158 (2016).
43. X. Li *et al.*, HSP27 attenuates cGAS-mediated IFN- β signaling through ubiquitination of cGAS and promotes PRV infection. *Viruses* **14**, 1851 (2022).
44. M. Chen *et al.*, TRIM14 inhibits cGAS degradation mediated by selective autophagy receptor p62 to promote innate immune responses. *Mol. Cell* **64**, 105–119 (2016).
45. Z. Ma *et al.*, Tegument protein UL21 of alpha-herpesvirus inhibits the innate immunity by triggering cGAS degradation through TOLLIP-mediated selective autophagy. *Autophagy* **19**, 1512–1532 (2022). [10.1080/15548627.2022.2139921](https://doi.org/10.1080/15548627.2022.2139921).
46. Y. J. Choe *et al.*, Failure of RQC machinery causes protein aggregation and proteotoxic stress. *Nature* **531**, 191–195 (2016).
47. D. Lyumkis *et al.*, Single-particle EM reveals extensive conformational variability of the Ltn1 E3 ligase. *Proc. Natl. Acad. Sci. U.S.A.* **110**, 1702–1707 (2013).
48. J. Chu *et al.*, A mouse forward genetics screen identifies LISTERIN as an E3 ubiquitin ligase involved in neurodegeneration. *Proc. Natl. Acad. Sci. U.S.A.* **106**, 2097–2103 (2009).
49. C. A. P. Joazeiro, Ribosomal stalling during translation: Providing substrates for ribosome-associated protein quality control. *Annu. Rev. Dev. Biol.* **33**, 343–368 (2017).
50. D. Lyumkis *et al.*, Structural basis for translational surveillance by the large ribosomal subunit-associated protein quality control complex. *Proc. Natl. Acad. Sci. U.S.A.* **111**, 15981–15986 (2014).
51. J. Cai *et al.*, USP7-TRIM27 axis negatively modulates antiviral type I IFN signaling. *Faseb J.* **32**, 5238–5249 (2018).
52. J. Zha *et al.*, The Ret finger protein inhibits signaling mediated by the noncanonical and canonical IkappaB kinase family members. *J. Immunol.* **176**, 1072–1080 (2006).